EUROPHYSICS LETTERS 20 January 1993

Europhys. Lett., **21** (3), pp. 329-334 (1993)

Structural Phase Transitions in C_{70}.

G. VAN TENDELOO(*), S. AMELINCKX(*), J. L. DE BOER(**), S. VAN SMAALEN(**) M. A. VERHEIJEN(***), H. MEEKES(***) and G. MEIJER(***)

(*) *Universiteit Antwerpen (RUCA)*
Groenenborgerlaan 171, B-2020 Antwerpen, Belgium
(**) *Laboratory of Chemical Physics, University of Groningen*
Nijenborgh 4, 9747 AG Groningen, The Netherlands
(***) *Research Institute of Materials, University of Nijmegen*
6525 ED Nijmegen, The Netherlands

(received 16 June 1992; accepted in final form 30 October 1992)

PACS. 64.70 – Phase equilibria, phase transitions, and critical points.
PACS. 61.16 – Other determination of structures.
PACS. 61.50 – Crystalline state (inc. molecular motions in solids).

Abstract. – Cubic as well as hexagonal single crystals of C_{70} have been grown and investigated by electron diffraction, electron microscopy and X-ray diffraction. Several phase transitions have been detected and crystallographic models are proposed. Hexagonal crystals, stable at room temperature with $c/a = 1.63$ will undergo two transitions, upon cooling. First the c/a ratio will increase to 1.82 owing to c-axis alignment of the molecules; at a lower temperature the molecules will orientationally order, resulting in a monoclinic structure.

The DSC curve of crystalline C_{70} exhibits two anomalies: a first one with onset at 276 K and a second one around 337 K [1]. The associated heats of transformation are, respectively, 3.5 J/g and 2.7 J/g; their sum (6.2 J/g) is closely equal to the heat of transformation of the orientational-ordering transition below 250 K observed in C_{60}. It is therefore reasonable to assume that also in C_{70} one or several orientational-ordering transitions occur in the mentioned temperature ranges. Little structural information is available on the crystalline phases involved in these transitions. It is the purpose of this paper to describe recent X-ray diffraction, electron diffraction and high-resolution electron microscopic observations, which give the first information on the crystallography of the low-temperature phases. Some of these results were already briefly reported earlier [2, 3].

The high-purity material (> 99.9% C_{70}) was prepared using well-established methods to produce solvent-free fullerenes. Extreme care was taken in growing crystals from the vapour phase; details on the preparation can be found in [2]. Even within the same batch two types of crystals were obtained. The majority of crystals had a multiply twinned cubic habit, a small number had a hexagonal habit. Room temperature electron microscopy of crystal fragments from both morphologies, obtained by crushing under liquid nitrogen, confirmed the crystal structures corresponding to their external habit. The cubic crystals had an FCC structure ($a = 1.46$ nm) containing planar defects; the crystals with a hexagonal habit were HCP stacked ($a = 1.06$ nm and $c = 1.73$ nm) with stacking faults as well.

In the hexagonal crystals, starting from a low-temperature orientationally ordered phase several phases are formed with increasing temperature by the successive excitation of

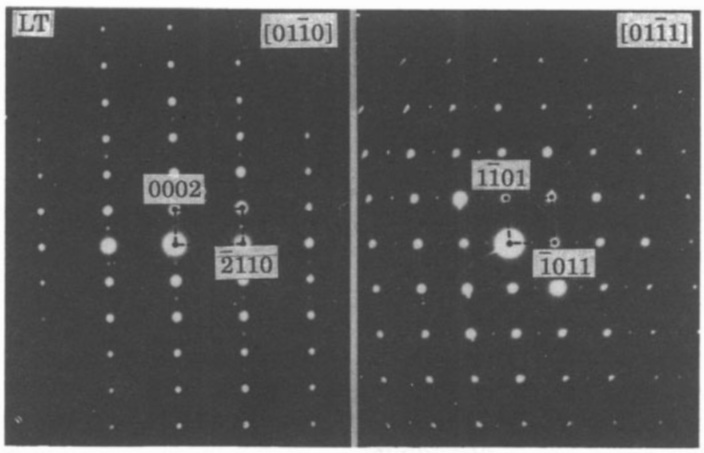

Fig. 1. – Electron diffraction patterns of the low-temperature phase of C_{70} for [01$\bar{1}$0] and [01$\bar{1}\bar{1}$], respectively.

rotational modes. We first describe the orientationally ordered structures of the low-temperature phase.

A first phase observed by electron diffraction at liquid-nitrogen temperature in hexagonal crystals produced diffraction patterns as shown in fig. 1. The indices refer to the hexagonal basic lattice. The intense spots must be attributed to the basic HCP structure. Weak supplementary spots occur for l = odd in sections in which such spots are systematically absent in the HCP diffraction patterns, which means that the normal diffraction conditions for the HCP structure are violated. Moreover, superstructure spots appear midway between the basic spots along rows parallel to [10$\bar{1}$1]*, but not in the rows parallel to symmetry-related directions, breaking in this way the hexagonal symmetry. The reciprocal lattice is represented schematically in fig. 2*a*); it is simply related to the reciprocal lattice of a hexagonal phase. The unit cell is monoclinic C-centred with $\beta = 120°$; the primitive unit cell is triclinic. The base vectors of the monoclinic lattice $\boldsymbol{a}_M$, $\boldsymbol{b}_M$ and $\boldsymbol{c}_M$ are related to the base vectors $\boldsymbol{a}_{1,H}$, $\boldsymbol{a}_{2,H}$ and $\boldsymbol{c}_H$ of the hexagonal parent structure by the relations

$$\boldsymbol{a}_M = \boldsymbol{a}_{2,H}\,, \qquad \boldsymbol{b}_M = 2\boldsymbol{c}_H\,, \qquad \boldsymbol{c}_M = 2\boldsymbol{a}_{1,H}\,.$$

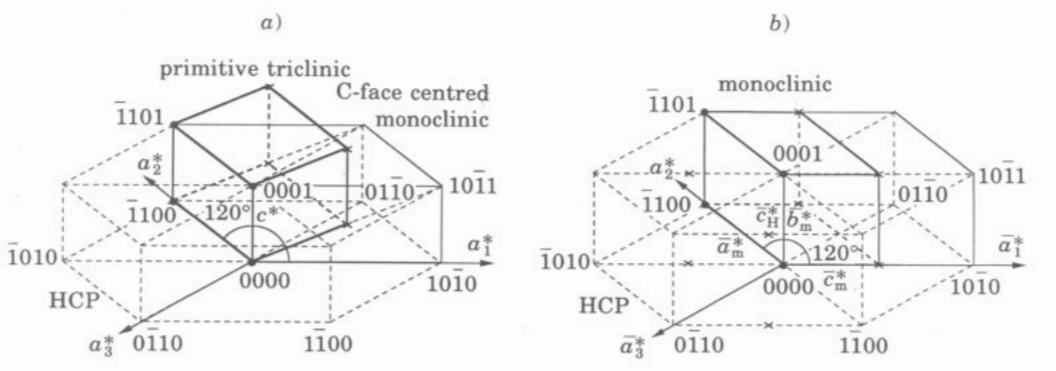

Fig. 2. – *a*) Reciprocal lattice of the monoclinic I phase as obtained from electron diffraction data. *b*) Reciprocal lattice of the monoclinic II phase as obtained from X-ray data and electron diffraction measurements.

There is, moreover a lattice point at $\boldsymbol{a}_{2,\,\mathrm{H}} + \boldsymbol{c}_{\mathrm{H}}$. The diffraction conditions are compatible with the space groups Cm and C2.

Four-circle single-crystal X-ray diffraction experiments as well as electron diffraction measurements made on a different hexagonal crystal have given evidence for the occurrence of a second, more abundant low-temperature phase. This phase gives rise to superstructure spots midway between the basic spots along all $[10\bar{1}0]_{\mathrm{H}}$ directions, related by hexagonal symmetry, but produced no evidence for a superperiod along the [0001]* direction. In view of the electron diffraction results, it is believed that the apparent hexagonal structure has in fact a primitive monoclinic lattice with a β angle of 120°, the a-parameter being doubled along one $[10\bar{1}0]_{\mathrm{H}}$ direction only. The base vectors of the monoclinic lattice are now related to those of the hexagonal parent structure by the relations

$$\boldsymbol{a}_{\mathrm{m}} = \boldsymbol{a}_{2,\,\mathrm{h}}\,, \qquad \boldsymbol{b}_{\mathrm{m}} = \boldsymbol{c}_{\mathrm{h}}\,, \qquad \boldsymbol{c}_{\mathrm{m}} = 2\boldsymbol{a}_{1,\,\mathrm{h}}\,.$$

The diffraction conditions are compatibile with the space group and $P2_1/m$. The reciprocal lattice of this second structure is represented in fig. 2*b*).

The two phases have closely related structures, both superstructures of the HCP structure. The superperiods originate from orientational ordering which makes the molecules in different sublattices distinguishable.

Assuming that the same stacking principle, which was found to determine the geometry of the orientationally ordered phase in C_{60}, also applies to C_{70}, we can propose a plausible model. The structure must be such that regions of high electron density of the molecules, *i.e.* along the 6-6 and 6-5 edges of the carbon cage, should face regions of low electron density of the adjacent molecules, such as the centres of hexagons or pentagons.

We first note that the c/a ratio of the ordered structure ($c/a = 1.83$) is approximately given by the ideal ratio for an HCP structure ($c/a = 1.63$) multiplied by the aspect ratio of the molecules. This shows that the molecules are stacked with their long axis parallel to the c-axis of the HCP structure. The stacking within the layers follows from the above- mentioned stacking principle. In a 2D close-packed parallel arrangement the molecules come closest to one another along their «equators». Along the equator of the molecule, which has fivefold rotation symmetry, five equally spaced high–electron-density regions along the 6-6 edges (indicated by + in fig. 3) alternate with five low–electron-density regions (indicated by − in fig. 3) situated in the centres of the hexagons. It is clear that a linear 1D arrangement in which all molecules have a parallel orientation strictly satisfies the stacking principle. The best (ideal) 2D arrangement is one in which successive rows of parallel molecules differ 180° in orientation, as represented in fig. 3 where the pentagons indicate the orientations. The stacking principle is now satisfied not only for molecules along one set of close-packed rows, but also to a good approximation among molecules in adjacent rows where + and − regions approximately face one another. It should be noted, however, that the 6-fold symmetry of a 2D close-packed arrangement and the 5-fold symmetry of the individual molecules are basically incompatible; therefore slight deviations of the 120° monoclinic angle are to be expected. This is the reason why a monoclinic description is preferred over an orthorhombic one.

The spatial arrangement of layers must be such as to give rise to a structure with the observed monoclinic unit cells. The stackings corresponding to the two described reciprocal lattices are shown in fig. 4. The letters A and B represent molecules differing 180° (or 36°) in orientation, situated in a-layers. Similarly A' and B' represent molecules in b-layers of the hexagonal *abab*... stacking. We cannot decide from the available evidence whether $A = A'$ and $B = B'$ or $A = B'$ and $B = A'$; both structural variants probably occur in both phases, since they are energetically equivalent. The structure contains four interpenetrating primitive monoclinic sublattices, each sublattice being occupied by molecules of a given orientation $A(A')$ or $B(B')$.

A single crystal of the basic hexagonal structure can give rise with equal probability to six orientation variants of the monoclinic structure, which are related by symmetry operations lost

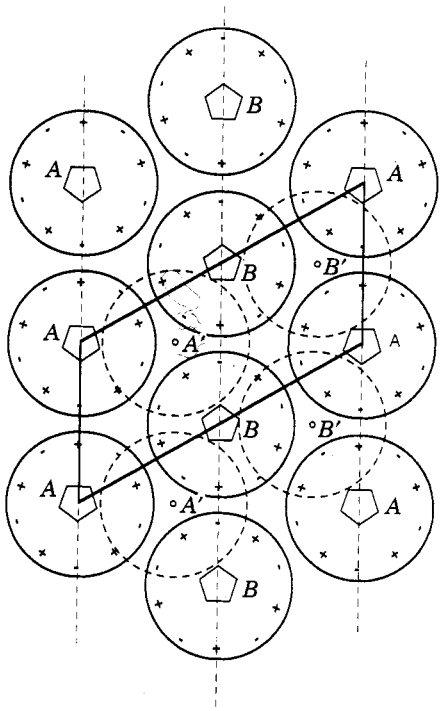

Fig. 3.

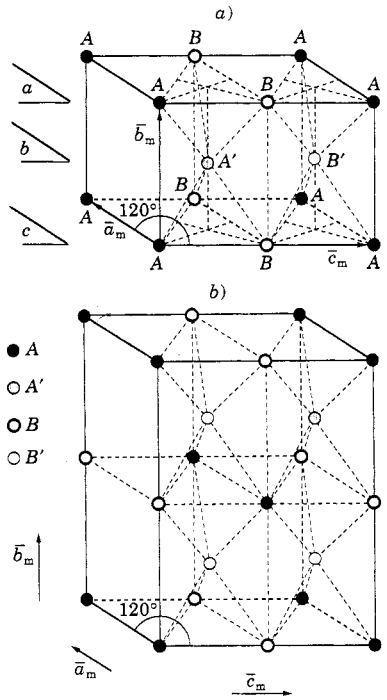

Fig. 4.

Fig. 3. – Basal-plane arrangement of C_{70} molecules in the low-temperature monoclinic phases. *A* and *B* refer to molecules rotated 180° with respect to each other; + and − signs indicate electron-rich and electron-poor areas along the equator of the molecule.

Fig. 4. – 3D arrangement of the stacking sequences of the monoclinic I (*a*)) and monoclinic II (*b*)) phases.

on ordering. The variant generating group is $3m$ of order 6 [4]. Each orientation variant can furthermore occur in translation variants, related by the lost translations of the HCP structure. On ordering this leads to extensive domain fragmentation, which will certainly hamper single-crystal X-ray studies.

We shall now describe how these structures gradually disorder with increasing temperature and present the relevant evidence. In a first step the rotations about the long axis of the molecules are excited. The diffraction evidence for this transition consists in the disappearence of the weak superstructure spots, with the conservation of a c/a ratio in the vicinity of 1.82. We call the corresponding structure HCP-1. In this structure the molecules have cylindrical symmetry, since they are freely rotating about their long axis. Such rotations are possible even for individual molecules, since there is no steric hindrance by neighbouring molecules.

The fragmentation of the low-temperature phase in orientation domains may become dynamical in nature when approaching the transition temperature of monoclinic to HCP-1. Domain boundaries can then easily move by the reorientation of molecules in the boundary. As a result it is to be expected that the transitions of the orientationally ordered structure into HCP-1 may proceed through an intermediate stage consisting of a fine texture of regularly arranged microdomains with mobile domain walls, and a temperature-dependent domain size. A somewhat similar effect to the domain fragmentation and the incommensurate phase is observed in quartz [5].

The next event with increasing temperature consists in a rather sudden decrease of the

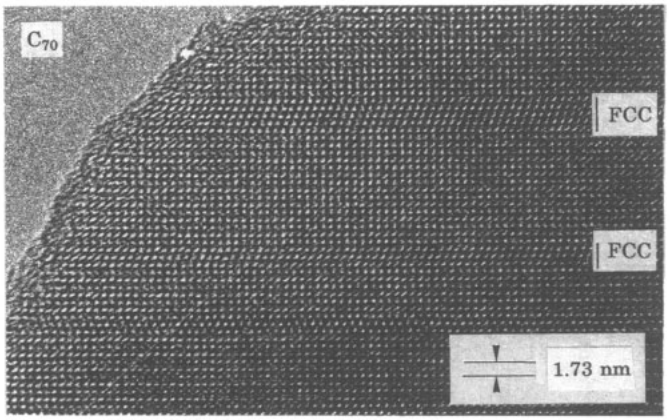

Fig. 5. – High-resolution image showing the interweaving of FCC and HCP bands.

c/a ratio to about $c/a = 1.66 \div 1.64$; we shall call this phase HCP-2. The decrease of the c/a ratio must be attributed to the excitation of rotational modes about axes other than the long axis. This can only take place cooperatively because of the steric hindrance; the transition is therefore rather sharp. Since the c/a ratio is still somewhat larger than the ideal value, there is still a slightly preferential orientation of the long axis parallel to $\boldsymbol{c}_H$. The effective shape of the models is now close to spherical.

The high-resolution observation (fig. 5) of an intimate mixture of faulted hexagonal and cubic stackings, at room temperature, is the signature of an incomplete shear transformation, which transforms the hexagonal stacking into a cubic one by the propagation of Shockley partials. The sense of the transformation, *i.e.* from *abab...* into *abcabc...*, can be deduced from the fact that faults occur on a single family of close-packed layers only; these are the $(0001)_H$ planes which become $(111)_C$ planes in the *abc* stacked phase. The structure of this phase is rhombohedral since the ratio, which is the analogue of the c/a ratio in the hexagonal structure, is found to be somewhat larger than the ideal value for FCC. The unit cell is thus an elongated rhombohedron with its threefold axis parallel to the hexagonal axis of the parent structure. The diffraction pattern along the $[001]_{FCC}$ zone shows that $\alpha = (88 \div 89)°$; it reveals directly the deviation from cubic symmetry. A slight increase in temperature, caused by increasing the electron beam current, is sufficient to make the crystal FCC. This transition is reversible, the sample can be cycled repeatedly between rhombohedral and FCC inside the electron microscope.

Due to the uncertainty on the specimen temperature during *in situ* cooling experiments we cannot specify the transition temperatures with accuracy. The succession of transitions is well established, however. Taking the results of Raman spectroscopy [6] together with our diffraction evidence, it is possible to propose a consistent picture; this is represented schematically in table I, which is a brief summary of our considerations. It proposes that the transition monoclinic–HCP-1 occurs at 276 K whereas the transition HCP-1–HCP-2 must probably be associated with the 337 K singularity in the DSC curves of ref. [1]. The shear transformation HCP-2–rhombohedral occurs over a broad temperature range somewhere above room temperature, but presumably already slowly at room temperature. We conclude this from the observation that a freshly prepared hexagonal powder sample transformed into a cubic one when left for several days at room temperature. This makes us believe that actually the cubic phase is the stable one at room temperature. A detailed discussion on the thermodynamic stability is not possible at this moment, also because the energy difference between the hexagonal and the cubic structure is undoubtedly very small.

It is furthermore found that samples which are cubically stacked as grown, usually do not transform into hexagonal on cooling. No superstructure is observed so far by electron diffraction

TABLE I. – *Schematic representation of the different phases occurring in* C_{70}.

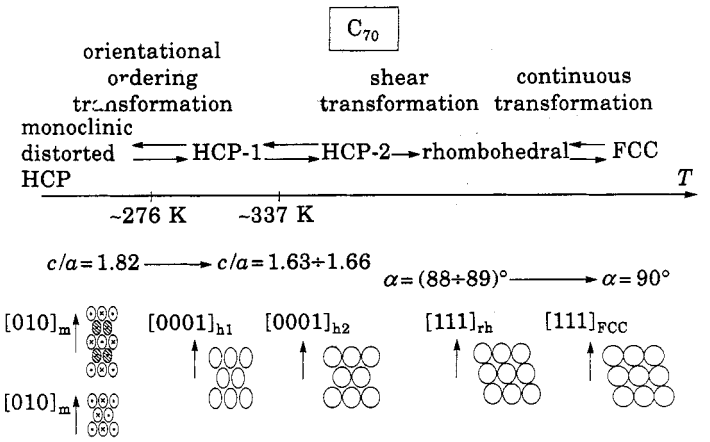

at liquid-nitrogen temperature in these crystals. We assume that at that temperature the cubic structure is presumably an orientational glass. The shear transformation is thus highly irreversible. This can be understood by noting that the shear transformation could now be nucleated with equal probability on four different families of (111) planes. The transformation partial dislocations in intersecting (111) planes presumably react and form stair-rod locks, preventing further transformation. It is also possible that the small particle size of the microscope samples hampers the nucleation of the hexagonal phase.

The present observations suggest a form of polytypism peculiar to the molecular crystals considered here. Within the same «positional polytype», in the present case within the same *abab* stacking, different orientationally ordered structures can be formed; we call them «orientational polytypes». There is clearly an interaction to be expected between positional faults (stacking faults in the basic structure) and orientational faults (faults in the molecular orientational pattern).

* * *

This work has been made possible with the financial help of the National Fund for Scientific Research (Belgium) and of the Services for Science Policy (IUAP 11) of the National Government (Belgium). Part of this work has been possible with the financial support of the Dutch Organisation for Fundamental Research of Matter (FOM) and the Netherlands Organization for Scientific Research (NWO/SON).

REFERENCES

[1] VAUGHAN G. B. M., HEINEY P. A., FISCHER J. E., LUZZI D. E., RICKETTS-FOOT D. A., MCGHIE A. R., HUI Y. W., SMITH A. L., COX D. E., ROMANOW W. J., ALLEN B. H., COUSTEL N., MCCAULEY J. P. jr. and SMITH III A. B., *Science*, **254** (1991) 1350.

[2] VERHEIJEN M. A., MEEKES H., MEIJER G., BENNEMA P., DE BOER J. L., VAN SMAALEN S., VAN TENDELOO G., AMELINCKX S., MUTO S. and VAN LANDUYT J., submitted to *Chem. Phys.*

[3] VAN TENDELOO G., AMELINCKX S., MUTO S., VERHEIJEN M. A., VAN LOOSDRECHT P. H. M. and MEIJER G., to appear in *Ultramicroscopy* (1992) and presented at the *Frontiers of Electron Microscopy in Materials Science, Oakland, April 21-24, 1992.*

[4] VAN TENDELOO G. and AMELINCKX S., *Acta Crystall. A*, **30** (1974) 431.

[5] VAN TENDELOO G., VAN LANDUYT J. and AMELINCKX S., *Phys. Status Solidi*, **33** (1976) 723.

[6] VAN LOOSDRECHT P. H. M. *et al.*, in preparation.